# Limit-Equilibrium Stability Analysis of Spiling Soil Reinforcement in Tunneling

S. BANG

ABSTRACT

A limit-analysis procedure for a spiling reinforcement system in soft-ground tunneling is described. The system is composed of a series of radially installed reinforcing spiles along the perimeter of the tunnel opening before excavation. The reinforcing spile network is extended into the in situ mass both radially and longitudinally. The system thus forms a temporary support with the advantage of not loosening the weak mass. It has been successfully used in weak rock formations as well as in soft ground on limited occasions. The limit-analysis formulation includes consideration of design parameters such as soil type and geometry of the tunnel and the reinforcing spiles. The procedure developed can be used to evaluate the overall stability or to determine the design parameters of the system or both.

In recent years underground construction has increased considerably as a logical part of the solution to many urban problems. Effective and safe underground excavation technology therefore has been sought to meet the challenge of this increasing demand.

On several occasions a spiling reinforcement system has been successfully used in tunneling to strengthen weak rock formations (1). On limited occasions the application also involved reinforcing tunnels in soft ground. The system typically consists of a series of radially installed reinforcing spiles 4.6 to 6.1 m long spaced between 0.6 and 1.5 m with an inclination angle of approximately 30 degrees to the tunnel axis. The reinforcing spiles are formed by inserting 2.5- to 3.8-cm diameter rebars into predrilled holes with subsequent grout. Figure 1 is a schematic representation of the system, the general principle of which is to stabilize a weak mass by installing an annular spiling reinforcement network along the perimeter of the tunnel heading before excavation. The reinforcing network is extended into the in situ mass both radially and longitudinally. The tunneling operation is therefore always performed inside a tubular reinforced zone encircling the tunnel opening.

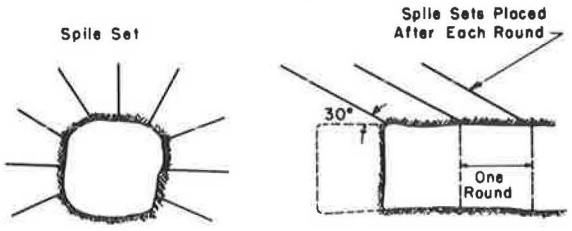


FIGURE 1 Spiling reinforcement system.

A limit-analysis procedure for the spiling reinforcement system in soft-ground tunneling is presented. The formulation includes consideration of design parameters such as soil type, depth and diameter of the tunnel, and length, inclination, and spacing of the spiles. The analysis procedure can be used to evaluate the overall stability of the system and to determine the proper size, spacing, and length of the spiles for a given site condition.

## BACKGROUND

The principle of the spiling reinforcement system is to strengthen the weak mass surrounding the tunnel excavation. The purpose is to improve the ground in terms of stand-up time by preventing loosening (immediate stabilization) and to contribute to permanent stabilization of the tunnel opening by restricting deformation.

Korbin and Brekke (2) conducted small-scale laboratory model tests to investigate the mechanism of spiling reinforcement in weak-rock tunneling. Behavior of cylindrical models with and without spiling reinforcement under uniform external pressures was examined. The study indicates that the system can stabilize a weak rock mass effectively by reducing deformations and thereby deterioration due to strain softening, providing increased available strength, and maintaining arching action, which allows for increased tangential stress in the immediate vicinity of the opening. Field instrumentation was also implemented at two sites (3). The investigation was designed to address questions related primarily to the magnitude, distribution, and time history of the deformation-induced tension and bending of the spiles as a result of excavation. Deformation-induced tension was found to be the major mechanism of the spiling reinforcement.

A generalized plane strain finite-element method of analysis was developed to investigate the behavior of the spiling reinforcement system in soft ground (4). The method of analysis developed was used to compare the results of the model tests conducted by Korbin and Brekke and was found very effective (5). The generalized plane strain condition assumes three nonzero displacement components, none of which is dependent on the out-of-plane coordinate; thus the out-of-plane strain remains zero instead of the out-of-plane displacement, as is commonly the case in the conventional plane strain approach. The main advantage of this approach is that it calculates three-dimensional stresses and

displacements, whereas the finite-element grid remains in two dimensions. A comprehensive parametric study to identify the effects of the various design parameters of the system was also conducted (6) by using the developed generalized plane strain finite-element method of analysis.

## LIMIT ANALYSIS AT EQUILIBRIUM

To date there have been no prototype failure studies of this system. Indirect methods therefore must be used to approximate the failure mechanism. As shown in Figure 2, contours of maximum shear strains were obtained from the previously described generalized plane strain finite-element analysis (6) and thus a potential failure surface can be approximated. The potential failure surface passes more or less through the side wall of the tunnel opening and propagates upward to form a curved surface. In this analysis the curved failure surface is approximated by two planes, defined by angles $\alpha_1$ and $\alpha_2$, with a change in direction at the back face of the reinforced zone as shown in Figure 2. A potential failure surface can then be determined by finding a set of angles $\alpha_1$ and $\alpha_2$ that yields the lowest overall factor of safety. Note that it is always assumed that $\alpha_1 \leq \alpha_2 \leq 90$ degrees.

### Formulation

Figure 3 shows the free-body diagrams of the assumed failure wedge. Because of the symmetry, only half of the failure wedge is considered. Forces acting on element 1 are $W_1$, $N_1$, $S_1$, $Q_1$, $N_3$ and $S_3$:

$$W_1 = \tfrac{1}{2}\gamma H_3^2 \cot\alpha_2$$
$$N_1 = \tfrac{1}{2}\gamma K_a H_3^2$$
$$S_1 = \beta N_1 \qquad (1)$$

where

W = body weight,

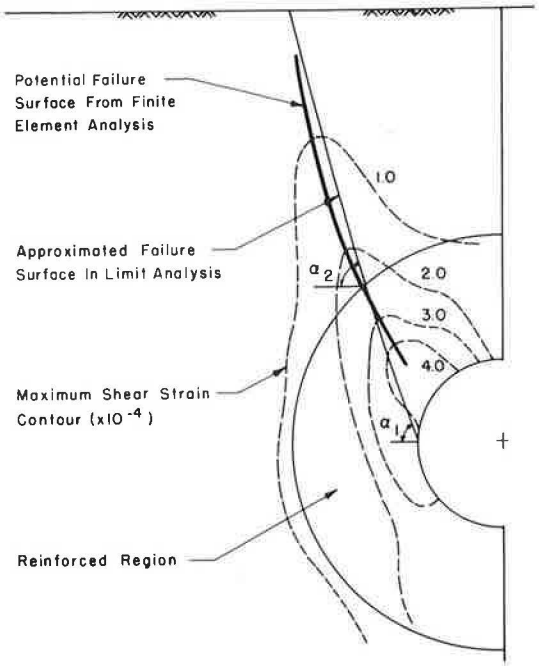


**FIGURE 2 Potential failure surface from contours of maximum shear strains.**

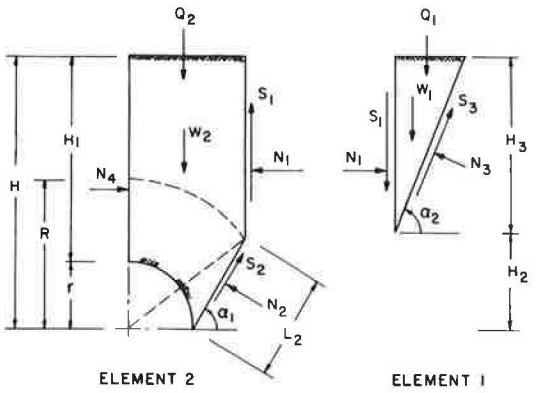


**FIGURE 3 Free-body diagrams of failure wedge.**

S = tangential force,
N = normal force, and
$K_a$ = active earth pressure coefficient.

The coefficient β describes the ratio between $S_1$ and $N_1$. Normal and tangential forces ($N_3$ and $S_3$) can be obtained from the equilibrium:

$$N_3 = (W_1 + Q_1 + S_1)\cos\alpha_2 + N_1 \sin\alpha_2$$
$$S_3 = (W_1 + Q_1 + S_1)\sin\alpha_2 - N_1 \cos\alpha_2 \qquad (2)$$

where Q is the surcharge.

The coefficient β can be obtained, on the assumption that the developed resisting force along the assumed failure surface is equal to the driving force; that is,

$$S_3 = C'(H_3/\sin\alpha_2) + N_3 \tan\phi'$$
$$= (W_1 + Q_1 + S_1)\sin\alpha_2 - N_1 \cos\alpha_2 \qquad (3)$$

where C' is the developed cohesion and φ' is the developed friction angle.

Substituting Equations 1 and 2 into Equation 3 yields

$$\beta = 2\{(W_1 + Q_1)\sin\alpha_2^2 - N_1 \cos\alpha_2 \sin\alpha_2 - C'H_3 - [(W_1 + Q_1)\cos\alpha_2 + N_1 \sin\alpha_2]\tan\phi' \sin\alpha_2\} \div K_a \gamma H_3^2 (\cos\alpha_2 \tan\phi' - \sin\alpha_2)\sin\alpha_2 \qquad (4)$$

Forces $W_2$ and $N_4$ acting on Element 2 are

$$W_2 = \gamma[H(r + L_2\cos\alpha_1) - (\pi r^2/4) - (H_2 L_2/2)\cos\alpha_1]$$
$$N_4 = \tfrac{1}{2} K_0 \gamma H_1^2 \qquad (5)$$

where

r = radius of tunnel,
$L_2$ = length of failure surface of Element 2, and
$K_0$ = at-rest earth pressure coefficient.

Note that the normal force acting on the plane of symmetry ($N_4$) is assumed to be the at-rest condition and that no shear force exists on the plane of symmetry. Force equilibrium of Element 2 yields

$$N_2 = (W_2 + Q_2 - S_1)\cos\alpha_1 - (N_1 - N_4)\sin\alpha_1$$
$$S_2 = (W_2 + Q_2 - S_1)\sin\alpha_1 + (N_1 - N_4)\cos\alpha_1 \qquad (6)$$

The driving forces of Elements 1 and 2 are $S_3$ and $S_2$, respectively, whereas the developed resisting forces of Elements 1 and 2 are

$$S_{R1} = C'L_1 + N_3 \tan\phi'$$
$$S_{R2} = C'L_2 + N_2' \tan\phi' + \sum_{n=1}^{m} T_{TT} \qquad (7)$$

where

$$N_2' = N_2 + \sum_{n=1}^{m} T_{TN},$$

$\sum_{n=1}^{m} T_{TN}$ = resultant of normal component of spile force $T_T$,

$\sum_{n=1}^{m} T_{TT}$ = resultant of tangential component of spile force $T_T$,

$T_T$ = component of developed spile axial force $T_n$ on X-Y plane,

$L_i$ = length of failure surface of element i, and

m = number of all spiles that cross assumed failure surface.

Figure 4 is the schematic representation of the spile force components.

## Resultant Forces in Spiles

It is assumed in this formulation that the spiles have the same length, inclination angle, and spacing. Neglecting the bending and shear as observed in field instrumentation (3), the maximum developed axial force in each spile ($T_n$) can be calculated.

Denoting stress tensors on X-Y-Z space and 1-2-3 space as $\underline{\underline{\sigma}}$ and $\underline{\underline{\sigma}}'$, respectively, where axis 1 is directed along the individual spile axis, one can obtain

$$\underline{\underline{\sigma}}' = \underline{\underline{A}}\,\underline{\underline{\sigma}}\,\underline{\underline{A}}^T \tag{8}$$

where direction matrix $\underline{\underline{A}}$ is defined as follows:

$$\underline{\underline{A}} = \begin{bmatrix} \cos\alpha & -\sin\alpha\sin\theta_n & -\sin\alpha\cos\theta_n \\ \sin\alpha\cos\theta_n & \cos\alpha & -\sin\alpha\sin\theta_n \\ \sin\alpha\sin\theta_n & \sin\alpha\cos\theta_n & \cos\alpha \end{bmatrix}$$

Angles $\alpha$ and $\theta_n$ are defined in Figure 4.

Stresses acting along the effective length of the spile (portion of the spile outside the failure wedge) can be assumed as

$$\sigma_y = \gamma Z_n$$
$$\sigma_x = \sigma_z = K_o \sigma_y \tag{9}$$

where $Z_n$ is the depth to the middle of the effective length of the nth spile. Therefore normal stresses acting on the spile ($\sigma_2$ and $\sigma_3$) can be calculated from Equations 8 and 9. The mean normal stress acting on the spile is then

$$\sigma_m = (\sigma_2 + \sigma_3)/2 \tag{10}$$

The resulting force in the spile is the developed frictional resistance; that is,

$$T_n = [\pi d\, \ell_n\, (\sigma_m \tan\phi' + C')]/S = A_S f_y \tag{11}$$

where

d = diameter of spile,
$\ell_n$ = effective length of nth spile,
S = spile spacing,
$A_S$ = spile cross section, and
$f_y$ = yield stress of spile.

The values of $\ell_n$ and $Z_n$ can be obtained from the geometry (Figure 5).

The projection of the nth spile on the X-Y plane forms an angle $\theta_n$ with the Y-axis, where

$$\cos^{-1}(H_2/R) \leq \theta_n \leq \pi/2 \tag{12}$$

From triangle OAB in Figure 5, it is obvious that

$$R_n^2 = r^2 + L_2^2 + 2\,r\,L_2\cos\alpha_1 \tag{13}$$

Because $R_n \cos\theta_n = L_2 \sin\alpha_1$, one can obtain

$$R_n = r[-B + (B^2 - 4A)^{1/2}/2A] \tag{14}$$

where

$$A = (\cos\theta_n/\sin\alpha_1)^2 - 1$$
$$B = 2(\cos\theta_n/\tan\alpha_1)$$

Therefore the effective length of the nth spile ($\ell_n$) and the depth to the middle of the effective length ($Z_n$) can be calculated; that is,

$$\ell_n = \ell - [(R_n - r)/\sin\alpha]$$
$$Z_n = H - [(R_n + R)/2]\cos\theta_n \tag{15}$$

where $\ell$ is the length of the spile.

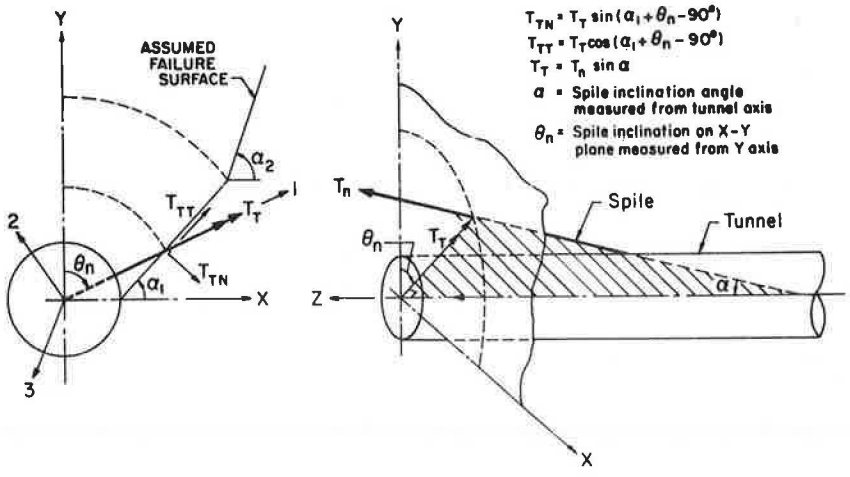


FIGURE 4 Forces in reinforcing spiles.

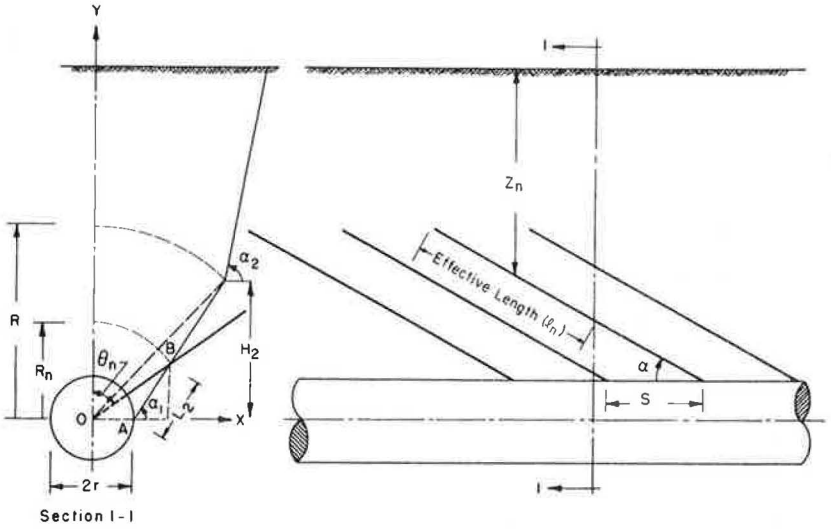


FIGURE 5 Geometric parameters.

EVALUATION OF OVERALL STABILITY

On the basis of Equations 3, 6, and 7, the overall stability of the system can be analyzed. At any stage, the driving force and the developed resisting force must be in equilibrium; that is, $S_3 = S_{R1}$ for Element 1 and $S_2 = S_{R2}$ for Element 2, or $S_2 + S_3 = S_{R1} + S_{R2}$. The overall factor of safety with respect to shear strength (FS) is defined as a factor of safety when $FS_c = FS_\phi = FS$ (7), where $FS_c$ is the factor of safety with respect to cohesion and $FS_\phi$ is the factor of safety with respect to friction.

The factor of safety with respect to cohesion or friction is the ratio between the available cohesion or friction and the developed cohesion or friction; that is,

$$C' = C/FS_c \text{ and } \tan\phi' = \tan\phi/FS_\phi$$

The overall factor of safety (FS) can then be determined. Because the expressions for driving and resisting forces contain an unknown FS, direct solution is not possible. An iteration method is therefore used.

A computer program was developed to calculate the overall factor of safety. For a given set of geometric and strength parameters, this program calculated the minimum overall factor of safety by searching a series of potential failure surfaces with different angles of $\alpha_1$ and $\alpha_2$. Typical results of this limit-equilibrium analysis are shown in Figure 6. The soil is silty clayey sand with an undrained strength of C = 19.15 kPa and $\phi$ = 33 degrees (8). The angle of spile inclination is 30 degrees to the tunnel axis in all cases. The results indicate that

1. The improvement in the factor of safety with respect to spile spacing is greater for longer spiles, and
2. The rate of increase in the factor of safety for a given spile length is greater for small spile spacings, as can be seen from the changes in slopes.

Figures 7 and 8 show the effects of tunnel depth and length and spacing of the spiles on the factor of safety. It is interesting to note that for a given spile length and spacing the factor of safety

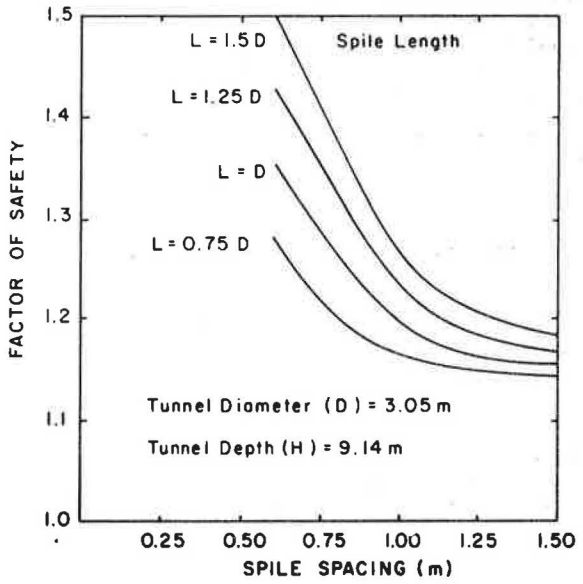


FIGURE 6 Typical results of limit analysis.

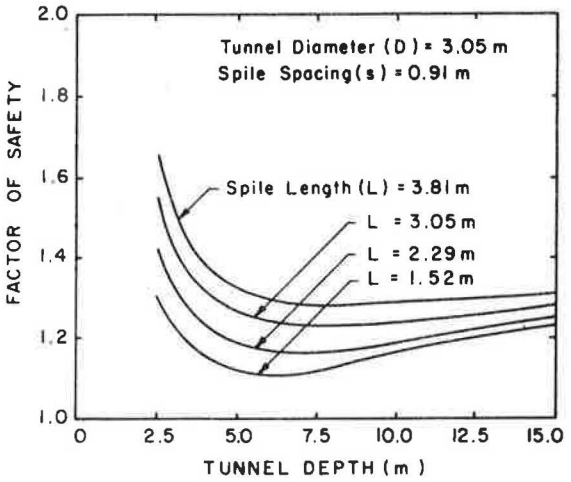


FIGURE 7 Effects of tunnel depth and spile length on factor of safety.

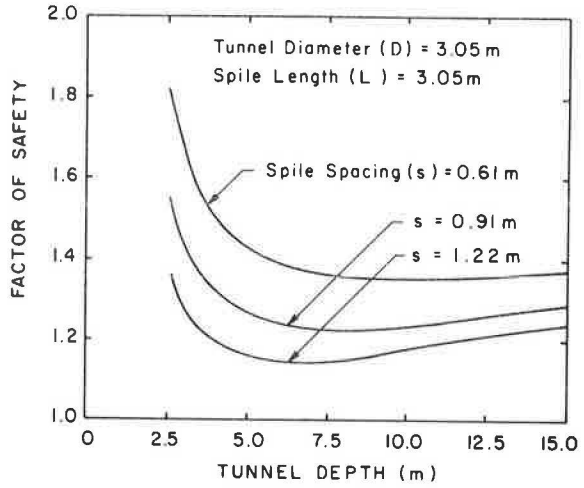


FIGURE 8 Effects of tunnel depth and spile spacing on factor of safety.

decreases as tunnel depth increases until a critical depth is reached. The factor of safety increases slightly below the critical depth. The rate of the decreasing factor of safety above the critical depth is, however, much greater than that of the increasing factor of safety below the critical depth. The critical depth is the location of the tunnel springline where the sliding tendency of the assumed failure wedge is maximum. The analysis is based on the equilibrium of driving and resisting forces along the assumed failure surface; therefore the factor of safety indicates a ratio between available soil strength and required soil strength mobilization against the sliding. Indeed the sliding tendency would be small at very shallow depths because of the small overburden and at greater depths because of arching.

## DISCUSSION AND SUMMARY

The stability analysis procedure of the spiling reinforcement system in soft-ground tunneling has been presented. A limiting stress equilibrium analysis has been performed to establish a design method for the system. The potential failure surface is approximated by two planes, starting from the side of the tunnel with a transition at the interface between the reinforced and unreinforced regions. The parameters found to be significant from the previous study are included in the formulation. Strength parameters, such as cohesion and friction, are assumed to be only partially developed, unless failure is imminent. From the equilibrium of the driving force and the developed resisting force, the overall factor of safety is obtained.

A comparison of the potential failure surface predicted by the finite-element analysis with generalized plane strain conditions was made with that predicted by limiting stress equilibrium analysis. Figure 9 shows one of the typical results. The agreement, though it has not yet been verified experimentally, between these two predicted curves is reasonably good.

The proposed formulation for the design of the spiling reinforcement system in soft-ground tunneling is intended to include the most essential characteristics involved in the system. However, a great deal of additional research is needed to describe the behavior of the system completely. Further research is necessary in areas such as field instrumentation and model testing to verify the analytical results.

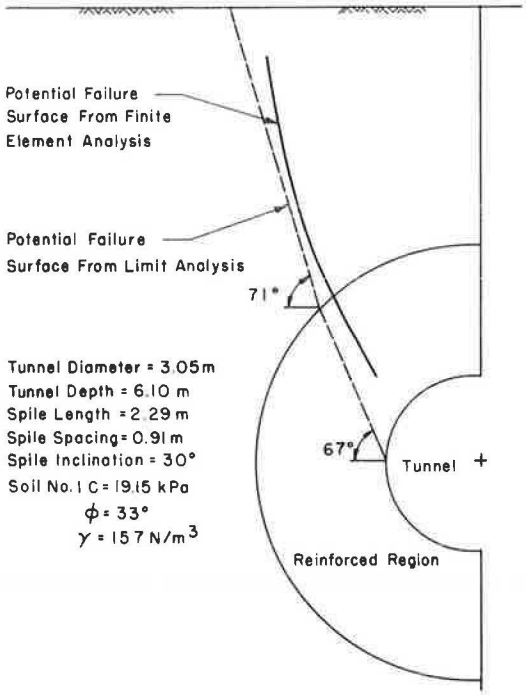


FIGURE 9 Comparison of potential failure surfaces.

## ACKNOWLEDGMENT

The research reported in this paper was supported by the U.S. Department of Transportation. The author is grateful for this support.

## REFERENCES

1. G.E. Korbin and T.L. Brekke. Model Study of Tunnel Reinforcement. Journal of the Geotechnical Engineering Division, ASCE, Vol. 102, No. GT9, 1976.
2. G.E. Korbin and T.L. Brekke. A Model Study of Spiling Reinforcement in Underground Openings. Technical Report MRD-2-75. Missouri River Division, U.S. Army Corps of Engineers, 1975.
3. G.E. Korbin and T.L. Brekke. Field Study of Tunnel Prereinforcement. Journal of the Geotechnical Engineering Division, ASCE, Vol. 104, No. GT8, 1978.
4. S. Bang. Analysis of a Spiling Reinforcement System in Soft Ground Tunneling. In Transportation Research Record 945, TRB, National Research Council, Washington, D.C., 1984, pp. 45-51.
5. S. Bang. Spiling Reinforcement System in Tunneling. Presented at 4th Australia-New Zealand Conference on Geomechanics, Perth, Australia, May 1984.
6. S. Bang and C.K. Shen. Soil Reinforcement in Soft Ground Tunneling. Research Report DOT/RSPA/DNA-50/83/5. U.S. Department of Transportation, Jan. 1983.
7. D.W. Taylor. Fundamentals of Soil Mechanics. John Wiley and Sons, Inc., New York, 1948.
8. J.M. Duncan, P. Byrne, K.S. Wong, and P. Mabry. Strength, Stress-Strain and Bulk Modulus Parameters for Finite Element Analyses of Stresses and Movements in Soil Masses. Report UCB/GT/80-01. University of California, Berkeley, Aug. 1980.

Publication of this paper sponsored by Committee on Subsurface Soil-Structure Interaction.